

A Chapter in the *Refractories Handbook*, edited by Charles A. Schacht, and to be published by Marcel Dekker, Inc., New York, NY 10016

Corrosion of Refractories

by

Denis A. Brosnan, PhD, PE
Clemson University
Clemson, SC 29634-0971

Introduction

Refractories are used at elevated temperatures for structural purposes and they are used in many cases to contain a high temperature corrosive environment. This corrosive environment usually contains liquid (melted) phases that participate in *chemical reactions* with the refractory at the elevated temperatures resulting in refractory consumption or wear. It is usually not immediately obvious, but the oxidation and reduction state of the environment (as “redox” conditions or oxygen “activity”) can participate in and influence the chemical reactions that take place. Along with chemical reactions during corrosion, *physical changes* occur that may be *accelerated by* the corrosion process.

Corrosion of refractories can be defined for the purposes of this discussion as follows:

Corrosion of Refractories – refractory wear by loss of thickness and mass from the exposed face of the refractory as a consequence of chemical attack by a corroding fluid in a process in which the refractory and the corroding fluid react approaching chemical equilibrium in the zone of contact between the refractory and the fluid.

It is an essential point that corrosion reactions proceed in a direction toward localized chemical equilibrium. This means that phase equilibrium diagrams can be used to analyze corrosion situations and to predict chemical strategies to minimize corrosion and wear rates. This gives persons interested in refractory corrosion two options. The first is to view corrosion as a chemical and physical process without a detailed application of phase equilibrium diagrams – called the “phenomenological approach”. The second is to use the information in the phenomenological approach *and* to use phase equilibrium diagrams. This latter option is required for a full understanding of refractory corrosion.

There are many types of refractory systems – fusion cast and/or bonded brick in a “working” lining placed in front of a backup or “safety” lining (or simply placed against a “shell”), thick-wall applications of concretes (and other monolithics) where the lining thickness is usually on the order of 75 mm or

greater, and thin-wall applications of monolithics where the lining thickness is typically less than about 25 mm. It is beyond the scope of this chapter to cover every type and application possible. There are fortunately a few fundamental principles that the investigator can apply to any corrosion situation, and it is a purpose of this chapter to provide those fundamental principles.

First Fundamental Principle on Refractory and Slag Compatibility

The first fundamental principle is that “acid” refractories tend to resist “acid” slags better than “basic” slags and, conversely, “basic” refractories tend to resist “basic” slags better than “acid” slags. The definitions of acidity and basicity in room temperature solution chemistry and of refractory chemistry at elevated temperature have a key difference:

Definition of Acidity and Basicity in Solution Chemistry at Room Temperature – an acid contains an excess of hydrogen ions (H^+) over hydroxyl ions (OH^-) considering a “baseline” defined as neutrality (a “pH” of 7.0). An acidic substance contributes hydrogen ions to a chemical solution to make it more acidic whereas a basic substance contributes hydroxyl ions to make it more basic.

Definition of Acidity and Basicity in Corrosion Chemistry at Elevated Temperature – an acidic material contains an excess of silica content (SiO_2) over basic materials (usually CaO) considering a “baseline” defined as neutrality (a CaO/SiO_2 ratio of 1.0). An acidic material contributes SiO_2 in a corrosion reaction whereas a basic material contributes CaO or MgO in a corrosion reaction.

This leads to the observation that acid refractories are more “compatible” with acid slags, i.e. acid materials experience less corrosion loss against acid slags as compared to basic slags. In a like manner, basic refractories are more compatible with basic slags than with acid slags.

In a strict definition of compatibility, mineral phases will not react at elevated temperature if they are compatible. This means on a microscopic basis, they will “stand beside” one another or coexist at equilibrium without reacting to form new substances. In general usage, the term “more compatible” just means “less reactive”.

There are more complex definitions of acidity and basicity for high temperature chemistry than those given above. For example, in steel refining the term “V” ratio is used where a ratio exceeding 1.0 implies a basic chemistry (usually a basic slag chemistry) and a ratio below 1.0 implies an acid chemistry. In definitions of this sort, the “V-ratio” can be expressed in terms such as the following:

$$V = \frac{\text{CaO} + \text{MgO} + \text{FeO} + \text{MnO} + \dots}{\text{SiO}_2 + \text{P}_2\text{O}_5 + \text{Al}_2\text{O}_3 + \text{Fe}_2\text{O}_3 + \text{Mn}_2\text{O}_3 + \dots}$$

In many cases, it is convenient to use three-component phase equilibrium diagrams in analyzing corrosion situations. The major refractory component can be visualized as one apex (corner) of the triangle with CaO and SiO₂ as the other components (apices). In these analyses, it is convenient to use the simple CaO/SiO₂ ratio. In more complex analyses using advanced thermodynamic software, it may be more accurate to use the V-ratio to define “equilibrium” conditions.

Corrosion reactions should be viewed as attempts by the system to achieve compatibility by progressing toward equilibrium. Refractories are rarely at chemical equilibrium on a microscopic scale since they are typically made from mixtures of different minerals. However, at the immediate corrosion interface between the refractory and the slag, the localized volume elements may be at or close to chemical equilibrium.

Second Fundamental Principle on Porosity and Corrosion Rates

Most refractories contain void space or porosity. This porosity may be open pores that can be penetrated by a fluid media (i.e. “apparent” porosity) and/or it may be closed porosity that is not easily penetrated by fluid media. If a refractory contained no porosity (or brick joints, expansion joints, or construction joints), the corrosion reaction is limited only to the face exposed to the corrosive media (called the hot face). When porosity is present, particularly when open porosity is present, the corrosive media can penetrate the refractory causing destructive reactions behind the hot face.

Most investigators have found that slag corrosion rates *increase linearly* with the percentage of apparent porosity within the refractory. This is usually true within a limited range of apparent porosity – for example in the range 12-16% apparent porosity – but it is not necessarily true at high apparent porosities (>20%).

It is for this reason that attention is directed toward achieving higher densities in refractories, i.e. obtaining the lowest possible apparent porosities. Higher density refractories usually exhibit lower wear rates. Understandably, very low-density refractories may exhibit less spalling resistance leading to higher wear rates by another process such as thermal shock. This points to the fact that corrosion loss is one part of many possible contributors to an overall wear rate for a furnace lining. Usually one wear process, such as corrosion, is the dominant wear process.

Because corrosive fluids can penetrate the refractory, such penetration usually results in disruption and even destruction of the “matrix” of the refractory. The matrix is the area of “sintered fines” that hold together “bonded” bricks and monolithic refractories. Usually, the matrix contains more impurities and more porosity than aggregate particles. Therefore, corrosion affects the “weakest” component of the refractory at a higher rate than more dense or higher purity particles. In extreme cases of matrix attack, rapid erosion of coarse refractory aggregate can occur.

Phenomenological Description of Corrosion

Introduction

The phenomena that occur during refractory corrosion are well known to anyone that has been around a furnace containing reactive process components such as slags or glasses. It is obvious that the reactive component, hereafter called the “slag”, must contact the refractory’s exposed surface or hot face at elevated temperature. It is at this interface that corrosion begins and continues throughout the life of the lining.

The situation is illustrated in considering a cross section of the slag and refractory interface (Figure 1). The refractory has a temperature gradient from the hot to cold face – meaning that the highest temperature is at the hot face and temperature declines across the refractory thickness toward its back or cold side. Slag is shown penetrating the refractory up until a “freeze plane” is reached. The freeze plane is the location in the refractory where the temperature is sufficiently low to cause the slag to solidify.

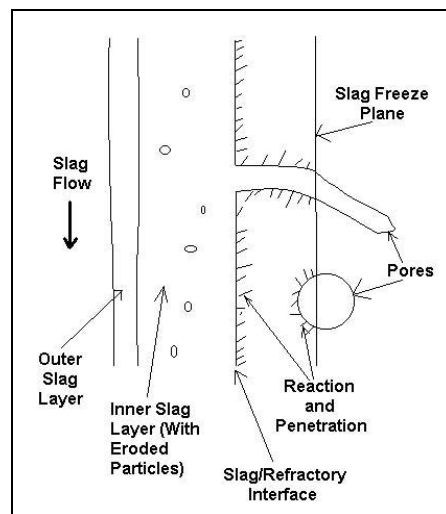


Figure 1: Cross Section of the Slag/Refractory Interfacial Area

The hot face of the refractory is coated with slag. In most metallurgical applications, this coating is relatively thin (~2-5 mm thickness). In some vertical wall refractory construction where the refractory is not in contact with a metal bath or slag pool, slag can accumulate in thick sections (>25 mm).

In some cases, two distinct slag layers can be observed on the outside of the refractory after a used material is sectioned. There may be a fluid “outer layer” over a “viscous appearing” inner layer with the latter directly contacting the surface of the refractory. The inner layer is typically influenced by solution of the refractory in the slag with the added components increasing the viscosity of the slag. There may be eroded particles of the refractory in the inner layer, which can be seen with the aid of a microscope. The two-layer situation is usually seen where liquid slag runs down a vertical refractory wall.

Two-dimensional representations in drawings or photomicrographs of the hot face zone cannot reveal the three dimensional structure underlying the area of the section. For this reason, pores appear that appear to be isolated, but they may be connected to the hot face through a channel under the observed plane. For this reason, pores that appear as isolated are many times filled with slag.

Slag reacts with the refractory forming new phases at the immediate hot face. Reaction also takes place behind the hot face where slag contacts the refractory at the pore walls. In metallurgical applications, metal can sometimes be seen penetrating the refractory along with slag.

Third Fundamental Principle on Reactions and Temperature Gradients

A key concept is that the temperature gradient affects the extent of phenomena seen in slag corrosion. In a very steep temperature gradient, very little penetration of slag is seen with corrosion reactions more or less restricted to the immediate slag and refractory interface. Mobility of fresh slag (reactant) to the slag/refractory interface may be limited, and transport of reaction products away from the slag/refractory interface may be slow. Steep gradients are seen in thin-wall refractory linings such as those used in utility boilers featuring water or steam cooling at the furnace shell.

In conventional refractory designs, the lining is at least one brick thickness (>225 mm), and the lining typically features a safety lining for a total thickness of at least 450 mm. The slag freeze plane may be located in a zone of 40-75 mm behind the hot face. In some cases, slag may penetrate up to 150 mm behind the hot face.

Thin Wall (Steep Temperature Gradient)

The corrosion situation in a thin wall refractory lining is illustrated in Figure 2. Here the refractory corrosion reactions occur primarily at the immediate hot face and there is little or no slag penetration. Microscopic examinations usually show that penetration is confined to a depth of less than 100 microns (0.1 mm) behind the exposed hot face. This situation may be called "Stage I" of slag attack where reactions occur at the immediate hot face.

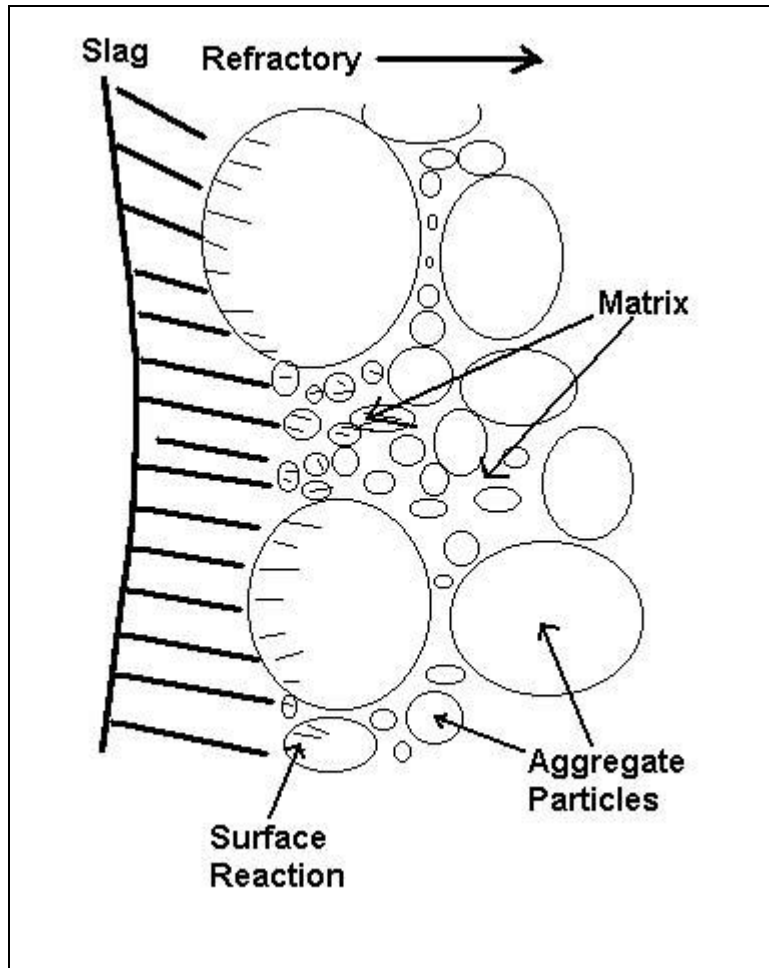


**Figure 2: Stage I of Slag Attack
(Showing a Bonded Refractory)**

It is found that the hot face temperature primarily affects the rate of corrosion reactions. If the hot face temperature is held just below the point that the products of corrosion become liquid (melt), corrosion will be very slow or non-existent. Most authorities believe that if the hot face is maintained at no more than 20°C above this melting temperature (called a lowest eutectic temperature),

reasonable corrosion rates will be observed. However, when the hot face temperature is more than 20°C above the eutectic, corrosion is rapid.

In some applications like utility boilers, “button fusion tests” are run to determine the slag melting temperature. A much more accurate test is to determine the eutectic or “solidus” temperature using thermal analysis. The solidus is recognized on heating with the appearance of an endothermic reaction (melting). The reaction temperature between slag and refractory can be determined by conducting a thermal analysis test of a mixture of ground refractory and ground slag.

Thin wall refractory designs rarely exhibit more extensive corrosion phenomena than are described as “Stage I” of corrosion. Therefore, the primary process variable affecting corrosion is hot face temperature. Secondary variables influencing corrosion rates include slag impingement velocity and slag chemistry. With respect to chemistry, the refractory will be soluble in the slag up to a certain extent (or percentage). If the slag is “satisfied” with respect to the chemistry of the refractory, slag corrosion should be minimal. The term “satisfied” means that the slag has reached the chemical solubility limit of major refractory constituents in the slag. Usually, the slag is not satisfied, i.e. it is corrosive. Attempts to make additions to the slag to obtain a satisfied chemistry (to minimize corrosion) are usually not economical.

There are a few cases of thick wall designs where the refractory is so resistant to slag corrosion that corrosion reactions are restricted to the hot face region. Usually these involve fusion cast refractories employed in furnaces that remain hot during their service life (minimal thermal cycling from hot to cold).

Thick Wall (Relatively Broad Temperature Gradient)

Thick wall refractory designs begin to exhibit corrosion on their initial coating of slag at elevated temperature. The initial process is Stage I of corrosion (Figure 2). Because of the broad temperature gradient, the refractory is penetrated by slag. Penetration is aided by capillary suction as the smallest pores in the refractory (diameter <10 microns) draw the liquid slag behind the hot face.

In time, extensive corrosion of the refractory takes place so that the refractory is at “Stage II” of corrosion (Figure 3). Stage II is characterized by two phenomena: (1) full penetration of the refractory and (2) extensive disruption by corrosion of the hot face region. Stage II follows Stage I only if there is a sufficiently broad temperature gradient to allow penetration.

In Stage II, the coarse aggregate in a bonded refractory exhibits penetration – particularly along grain boundaries (boundaries between crystals

making up polycrystalline aggregate particles). The direct bonding between the matrix and the aggregate particles is disrupted, but this bonding still exists.

Slag penetration in Stage II can result in densification spalling. This type of spalling occurs because the thermal expansion coefficient in the slag penetrated zone is different than that in the unpenetrated cold face region. On continued thermal excursions (cooling and heating), spalling can occur at the line of demarcation between penetrated and unpenetrated areas. The residual lining, after spalling, then begins the corrosion process anew progressing from Stage I to Stage II again.

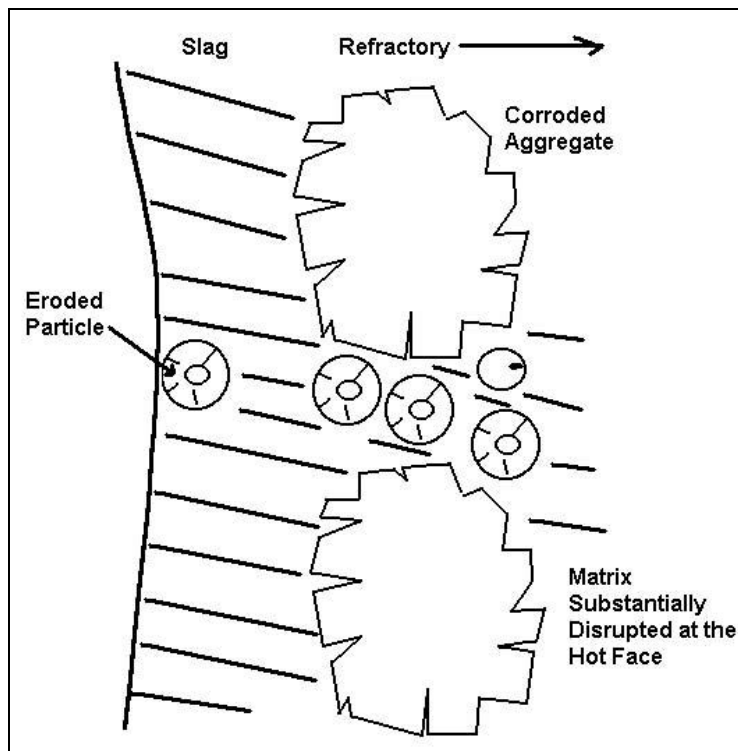


Figure 3: Stage II of the Corrosion Process (Showing a Bonded Refractory)

Toward the end of the life of the refractory lining or in cases of relatively slow corrosion rates and where densification spalling has not taken place, the refractory hot face zone may progress to a final stage of corrosion that may be called "Stage III" (Figure 4). In this case, bonding in the hot face region and up to 2-4 mm behind the hot face is minimal. The slag itself "appears" to be the only phase holding the residual aggregate particles in place. This is probably a result of the higher viscosity of the slag in the hot face region created as a consequence of dissolution of the refractory in the slag.

Because of the influence of slag viscosity maintaining some coherence in the hot face zone in Stages II and III with thick wall designs, a key process variable affecting corrosion rate is hot face temperature. Many investigators

recommend a hot face temperature not more than 20°C above the solidus temperature between the slag and the refractory. Such temperature restrictions are impractical in many thick wall refractory designs.

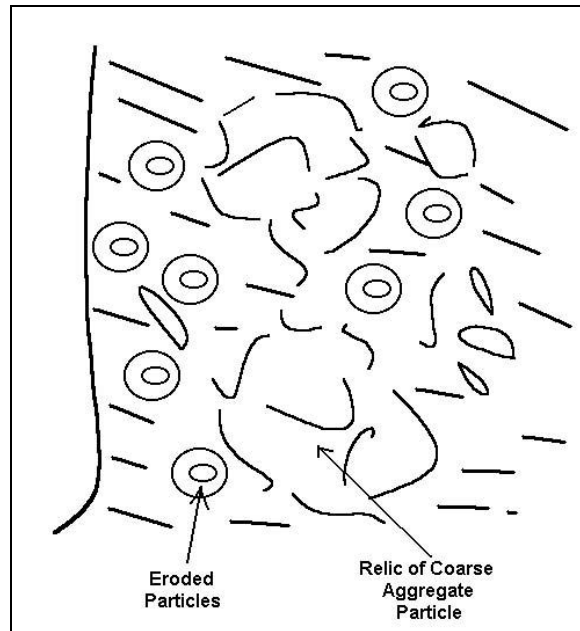


Figure 4: Stage III of the Corrosion Process

Equilibrium Considerations and Phase Diagrams

A phase diagram is a map showing equilibrium phases present as a function of composition and temperature. The phase diagram essentially shows the melting relationships in a given chemical system. It is beyond the scope of this chapter to provide a detailed description of phase diagrams and their interpretation (Burgeron and Risbud).

Even without a complete understanding of phase diagrams, they can be used in a “simplified method” to analyze corrosion. This method provides a “first approximation” of the corrosion potential of the system. This technique will be illustrated using the $\text{Na}_2\text{O}-\text{Al}_2\text{O}_3-\text{SiO}_2$ system (Figure 5). In the chapter on Alumina-Silica Brick, two consequences of Na_2O exposure were mentioned for alumina-silica brick including “glazing” (corrosion to form melted phase) and expansions. This discussion will only consider corrosion of the refractory to form liquids during corrosion.

The *first step* is to locate the point on the diagram representing the refractory main constituents. For this discussion, we will use a 40% Al_2O_3 superduty brick in contact with a corrosive phase consisting of 20% Na_2O and 80% SiO_2 . Both of these compositions are indicated in Figure 5 with a blue dot

indicating the approximate composition of the slag and a green dot indicating the approximate composition of the brick (on the Al_2O_3 - SiO_2 composition line or “join”).

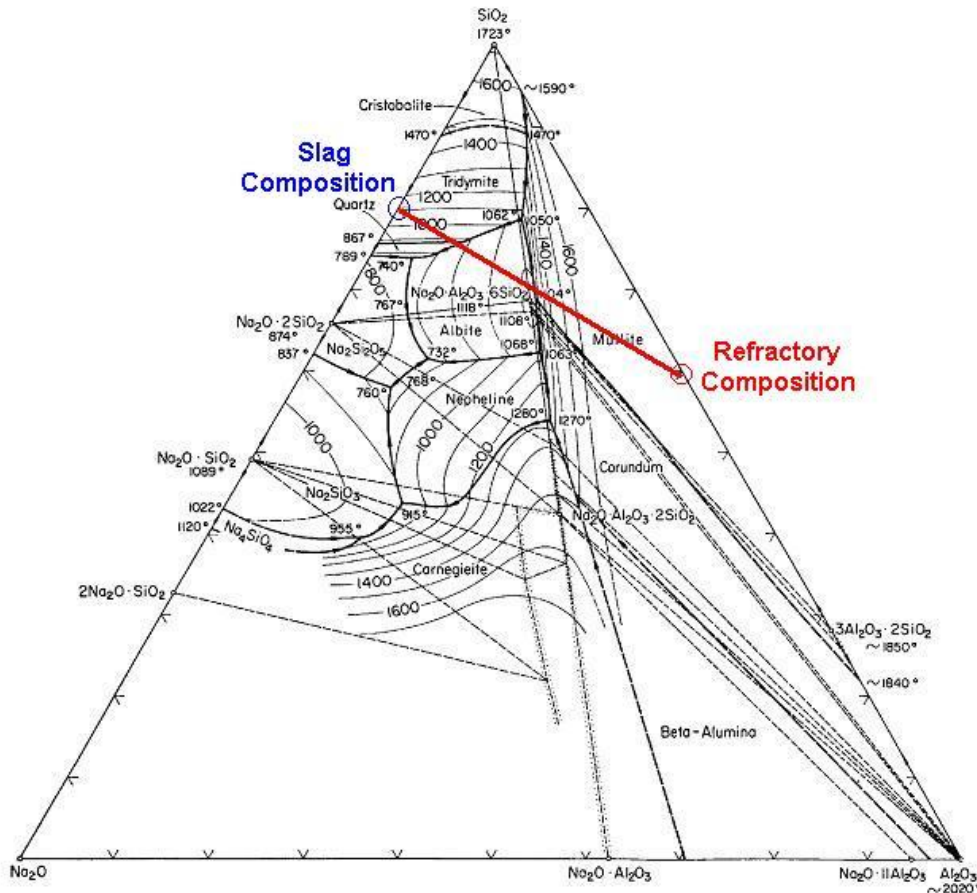


Figure 5: Na_2O - Al_2O_3 - SiO_2 Phase Diagram Used in A Corrosion Example

The second step is to draw a line between the slag composition and the brick composition (indicated in red in Figure 5). It is *essential* to recognize that all potential reaction products between the refractory and the slag at equilibrium must be located on the red line in Figure 5.

The analysis of the corrosion potential is as follows:

1. At the slag/refractory interface, the composition must move from that of the refractory in a direction toward the composition of the slag, i.e. the local composition moves in a “northwesterly” direction.
2. The compound at equilibrium between the slag composition and the refractory composition is “albite” or $\text{Na}_2\text{O} \cdot \text{Al}_2\text{O}_3 \cdot 6\text{SiO}_2$, melting at 1104°C . Therefore, at equilibrium, the localized melting point of corrosion products at the hot face is 1104°C . Note that albite is contained in the “compatibility” triangle between SiO_2 , mullite ($3\text{Al}_2\text{O}_3 \cdot 2\text{SiO}_2$), and albite.

The compatibility triangle establishes the phases that may be present at equilibrium. Mullite and SiO_2 (as glass or vitrified phase) are intrinsic to the refractory. Albite is formed as a consequence of corrosion reactions.

3. The red line joining the refractory and the slag crosses temperatures as low as about 1000°C . This implies that non-equilibrium liquids could be formed at this low temperature during corrosion. In Stage I of corrosion, such non-equilibrium liquids are expected. Only in Stage II of corrosion will sufficient refractory be dissolved in the slag to allow observation of the equilibrium corrosion product.
4. The red line joining the refractory and the slag composition crosses the $\text{Na}_2\text{O}\cdot 2\text{SiO}_2 - \text{SiO}_2 - \text{Na}_2\text{O}\cdot \text{Al}_2\text{O}_3\cdot 6\text{SiO}_2$ compatibility triangle near the ternary (3-component) eutectic or lowest melting temperature of 740°C . This implies liquids melting as low as 740°C could be formed during non-equilibrium conditions.

Considerable qualification is needed when performing this type of analysis. One is that the refractory contains other components than Al_2O_3 and SiO_2 – notably fluxes like K_2O and Fe_2O_3 . These components can lower the melting points predicted by the diagram. Additionally, the slag may contain other components changing the melting relationships. The analysis still has considerable value for use in a first approximation.

Selected Models for Slag Attack on Refractories

Konig's Model

In 1971, Konig related the corrosion rate of refractories in bosh area of blast furnace walls to the temperature gradient in the wall. This analysis includes an assumption that the temperature gradient controls the temperature at the slag/refractory interface (See Figure 6 where the interface temperature is labeled T_s). Because the shell of a blast furnace is water cooled in the area of the bosh, Konig's analysis is appropriate for thin wall refractory with a steep temperature gradient fixed by the process (furnace) temperature and cold face temperature

Konig created a heat balance by assuming that the heat flux into the refractory surface must equal the heat flux through the furnace shell. If the heat flux into the refractory surface exceeds the heat flux out of the shell, the interface temperature (T_r) must increase causing increased corrosion rates until the heat balance is maintained once again. Terms used in Konig's analysis are given in Table 1.

The slag/refractory interface temperature becomes T_c (critical temperature) when the heat flux into the refractory equals the heat flux out of the shell. In other words, T_c is an "equilibrium thickness" in the lining. If the actual

temperature is above T_c , rapid corrosion (recession) of the refractory is expected until a dynamic equilibrium is once again achieved.

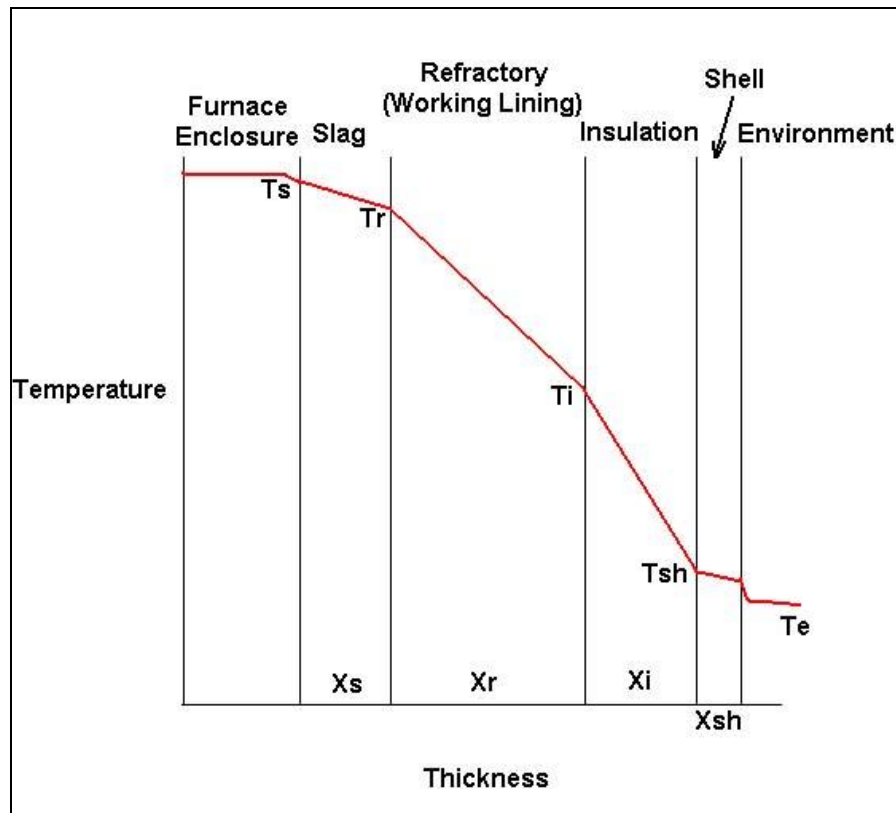


Figure 6: Konig's Thermal Model

Term	Definition
Q_1	Heat flux into the refractory surface.
Q_2	Heat flux through the furnace shell.
A	Area of the exposed refractory in the furnace.
t	Time at elevated temperature.
T_i	Temperature where i =slag surface(s), refractory/slag interface(r), insulation hot face(i), or shell(sh).
x_i	Thickness of component where i =slag layer(sl), refractory working lining(r), insulation(i), or shel(sh).
k_i	Thermal conductivity where i =refractory working lining(r), insulation(i), or shell(sh).
T_c	Critical temperature at the slag/refractory interface.
f_i	A film coefficient for convective heat transfer where i = furnace environment (F) or room environment (E).

Table 1: Terms Used in Konig's Analysis

The heat flow into the refractory surface is described by the equation:

$$Q_1 = f_F A t (T_F - T_s)$$

The heat flux out of the furnace shell is:

$$Q_2 = k_{\text{eff}} A t (T_r - T_E)$$

where k_{eff} is the effective (overall) thermal conductivity through the refractory, insulation, shell, and film contribution in the room environment.

From heat transfer theory, the relationship for k_{eff} is:

$$k_{\text{eff}} = \frac{1}{f_E + \frac{x_r}{k_r} + \frac{x_i}{k_i} + \frac{x_{sh}}{k_{sh}}}$$

At equilibrium, $Q_1 = Q_2$ and $T_r = T_c$, so that algebraic manipulation provides a relationship for the "equilibrium thickness" (x_r) of the working lining as:

$$x_r = k_r \left[\frac{1}{f_F} \times \frac{(T_c - T_E)}{(T_F - T_{sl})} - \left(f_E + \frac{x_i}{k_i} + \frac{x_{sh}}{k_{sh}} \right) \right]$$

Konig's relationship for the equilibrium thickness provides the following insight:

- The equilibrium thickness x_r increases linearly as the thermal conductivity of the refractory increases.
- The equilibrium thickness x_r increases as the thermal conductivity of the insulation increases. This is why conductive ramming materials are used behind high thermal conductivity basic refractories to insure the best possible cooling effect of the shell.
- The equilibrium thickness x_r increases as the T_c of the refractory/slag system increases, i.e. as more slag resistant refractories are used. This usually means use of higher purity refractories, i.e. higher alumina content or higher MgO purity.

- The equilibrium thickness x_r changes as the heat transfer into the lining or out of the shell changes, i.e. as the film coefficients change.

In attempts to apply Konig's analysis to the blast furnace, Herron and Beechan found that corrections were necessary if the refractory's thermal conductivity changes dramatically with increasing temperature. The model was found to describe the behavior of refractories in cyclone burners and in boiler applications where the initial wall thickness of refractory was ~25mm.

The Model of Endell, Fehling, and Kley

In a classic reference, Endell, Fehling, and Kley developed an empirical relationship for slag corrosion in a thick-walled refractory lined vessel with slag flowing down a vertical refractory wall. While this work was performed in 1939, it remains the classic reference on slag corrosion despite its empirical nature. In the corrosion studies, the authors used an arrangement where a solid fuel burned within a reaction chamber (liberating heat) with resulting ash (slag) impingement on walls. Terms used in the analysis are given in Table 2.

Term	Definition
R	Slag attack rate, i.e. refractory recession, in cm/s.
L_o	Solubility of refractory in slag in kg of refractory/kg of slag.
T	Absolute temperature of the refractory hot face.
η	Slag viscosity in poises.
f	Fraction of ash adhering to the refractory wall – interpreted as slag impingement.
H	Heat liberated in the furnace chamber in kcal/m ³ -hr.
A	Ash content of the fuel in grams pf ash.
C	A constant for the furnace geometry.

Table 2: Terms in the Analysis of Endell, Fehling, and Kley

The mathematical relationship for slag attack rate is:

$$R = CL_o \left(\frac{T^{2/3}}{\eta^{8/9}} \right) (HA)^{1/6}$$

The empirical model of Endell, Fehling, and Kley for thick wall refractory linings provides the following information:

- There is a *very strong dependence* of refractory corrosion rates on *hot face temperature*. In fact, temperature is the most important process variable that can be considered in furnace design or process control.
- The slag attack rate *increases linearly* with the *solubility of the refractory in the slag*. While modern high Al_2O_3 or high MgO products were not included in the original research, modern practices have shown that corrosion rates can be reduced if the slag chemistry is adjusted to reduce solubility of the refractory in the slag.
- In essence, the corrosion rate is inversely proportional to slag viscosity. This is probably why refractories exhibit some coherence in Stage III of slag attack because solution of refractory in the slag has increased viscosity at the slag/refractory interface.

In their concluding remarks, Endell, Fehling, and Kley recommend maintaining a hot face temperature of no more than about 30°C above the solidus or eutectic temperature between the refractory and slag. The authors further recommend that a temperature gradient in thick wall linings should not exceed $10^\circ\text{C}/\text{cm}$ or $50^\circ\text{F}/\text{in}$. While these criteria are difficult to maintain given the other purposes for furnaces in processing, they establish criteria for reducing corrosion rates.

Case Studies of Corrosion

Alumina-Silica Brick in Ferrous Foundry Applications

Introduction

Slag used in ferrous foundry applications is found to contain lime (CaO), silica (SiO_2), iron oxide (FeO), and other oxide constituents. *As a first approximation*, the slag can be assumed as a binary mixture of alumina and silica as they are usually the major components of the slag. The major components of the brick can be represented using the binary Al_2O_3 - SiO_2 phase diagram, and this allows the corrosion situation to be analyzed using the three-component CaO - Al_2O_3 - SiO_2 phase diagram (Figure 7).

Cases of corrosion of 70% Al_2O_3 and 90% Al_2O_3 brick are analyzed below using Figure 7. The composition of the brick is plotted on the Al_2O_3 - SiO_2 binary (2-component) side of the diagram. Then a line is drawn to the expected slag

composition using the average CaO/SiO₂ ratio of the slag. For this discussion, the slag is assumed to have a CaO/SiO₂ ratio of ~1.0.

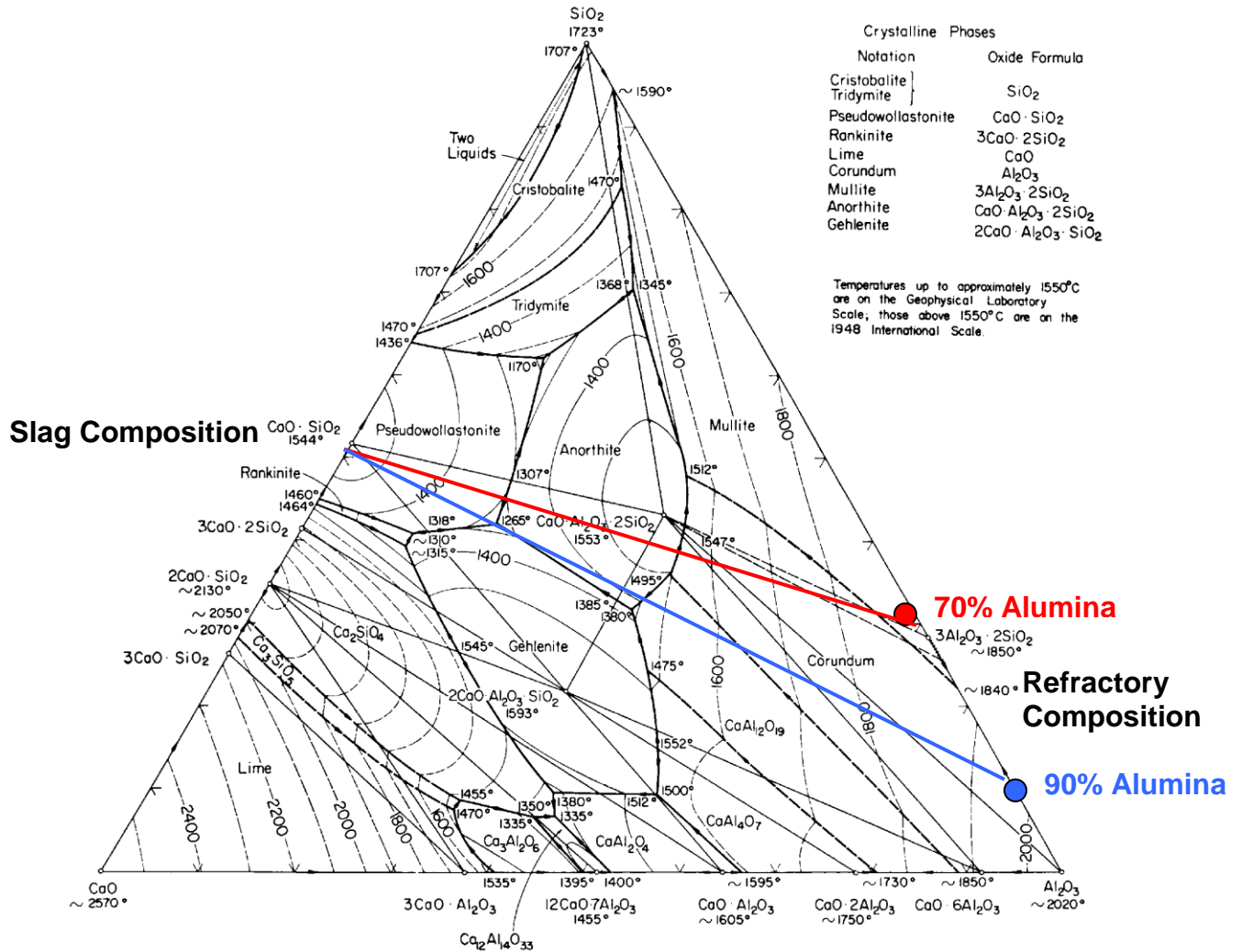


Figure 7: Representation of Corrosion of Alumina-Silica Brick In Foundry/Steel making Slag

A few things are very clear on looking at the lines joining the brick composition and the slag composition in Figure 7:

- Both “joins” between brick and slag pass very close to the ternary eutectic at 1265°C implying that the slag and refractory compositions will produce liquid phases, i.e. exhibit corrosion, whenever they are in intimate contact

and when this temperature is reached. Other fluxing oxides typically reduce this temperature by as much as 50°C.

- The effect of lime (CaO) – rich phases penetrating the brick is to render the mullite “binder” in the refractory as a non-equilibrium phase, i.e. the binder is dissolved into the penetrating slag phases and corrosion products. In 70% Al₂O₃ brick, the mullite is stable until the local composition reaches ~20% CaO, while in 90% Al₂O₃ brick the mullite disappears when the local composition reaches ~8% CaO.

The phase diagram has provided a first approximation of the reaction temperature between the slag and refractory for corrosion to begin, i.e. when liquid phase is produced as a product of corrosion reactions. This is analogous to the critical temperature in König’s analysis or the ‘baseline’ temperature in the analysis of Endell, Fehling, and Kley.

The joins between refractory composition and slag composition in Figure 7 could have been constructed to analyze the situation with higher slag basicity, i.e. CaO/SiO₂ of 1.5 or 2.0. In this situation, the lines would cross close to the ternary eutectic at 1380°C. This eutectic mixture between anorthite and gehlenite has the special name of “melilite”. The binary join between anorthite and gehlenite is shown in Figure 8, where it is easier to see the solidus temperature, i.e. the temperature above which corrosion begins. Thus, higher CaO-SiO₂ ratios increase the initial reaction temperature between the slag and refractory with respect to formation of liquid phases and the beginning of corrosion.

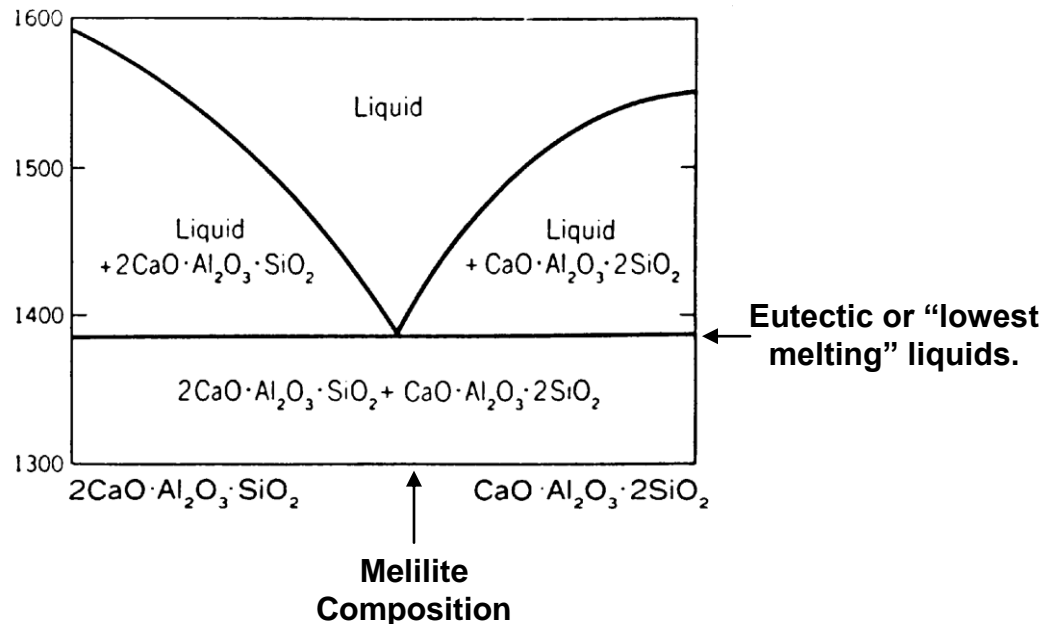


Figure 8: Binary Phase Diagram Between Gehlenite (2CaO·Al₂O₃·SiO₂) and Anorthite (CaO·Al₂O₃·2SiO₂)

Case Study: 70% Al₂O₃ Brick In An Electric Arc Furnace Roof

A microscopic study of 70% alumina brick after service in the roof of an electric arc furnace was performed to determine the reason for a premature failure of the brick in the roof. Several pieces of brick after service exhibited minimal thickness (Figure 9). In brick selected from other areas of the roof, a greater residual thickness of brick was observed. Cracks were found on saw-cut surfaces of most used brick from this furnace campaign, and cracks were arranged approximately parallel to the hot face.

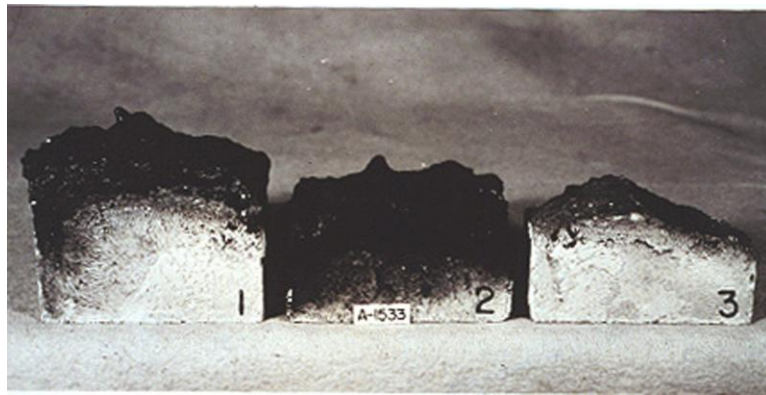


Figure 9: 70% Alumina Brick After A Short Arc Furnace Campaign

The bricks were sectioned, and polished sections were produced for reflected light examination on an optical microscope. In the area of the immediate hot face, i.e. at the slag/brick interface, there was ample evidence of corrosion reactions (Figure 10). Recognizing that the “native” phases in the brick are bauxite, clay (grog), and mullite, there is no mullite visible at the immediate hot face. Phases in the hot face in Figure 10 include hercynite or FeAl₂O₄ (labeled “S”), calcium hexaluminate or CaO·6Al₂O₃ (light gray needles), lath-like corundum crystals exsolved from the liquid on cooling, corundum crystals (Al₂O₃) in a relic bauxite grain (lower right field), and a dark gray background of calcium aluminosilicate glass.



Figure 10: Microstructure at the immediate Slag/Brick Interface (130X)

At a position of about 2-4 mm behind the hot face, slag penetration has taken place through the pore structure of the brick, and the position where mullite crystals appear was easily noticed because of their extreme crystal growth (Figure 11). The mullite crystals are seen as large light gray laths at a pore wall surrounded by relic bauxite grains. Small calcium hexaluminate crystals are located in the glass phase between mullite crystals.

The appearance of mullite signifies the position where the CaO content of the penetrating phase is below about 20%. This is a consequence of the “dilution” of the slag by the corrosion of the brick and the lesser amount of slag as distance is traversed away from the hot face.



Figure 11: Position Where Mullite Crystals Appear Behind The hot Face

At a position of about 10 mm behind the hot face of the brick, slag penetration stopped. Near the cold face of the brick, the microstructure of the brick was normal for a 70% Al_2O_3 brick product made using a mixture of calcined bauxite and clay. The conclusion from this study was that the normally expected corrosion reactions were found to take place, and the accelerated wear was likely due to poor thermal shock resistance resulting in enhanced spalling that ultimately shortened the campaign of the electric furnace roof.

In summary, the corrosion processes for the 70% Al_2O_3 brick were:

1. Slag coated the surface of the hot refractory, and corrosion began as the surface temperature exceeded about 1265-1380°C. The reaction can be expressed in words as: “calcium (iron) alumino-silicate slag reacts with 70% alumina refractory forming a gehlenite-anorthite glass with solution of mullite and bauxite in the slag”.
2. Slag penetrated the refractory filling the pores with liquid and dissolving the bond phase (mullite) until the local CaO content of the slag dropped below about 20%. Behind this area, mullite reappeared and exhibited crystal growth to a progressively lower extent until the freeze plane for slag in the brick was attained.

Case Study: 90% Al_2O_3 Brick From A Metal Contact Zone
In a Ferrous Foundry Furnace

In another case study involving a different foundry, 90% Al_2O_3 brick were examined for evidence of corrosion after service in a ferrous foundry furnace hearth/lower sidewall application. The premature failure was in a “skewback” brick at the furnace hearth that was supporting the lower furnace sidewalls. A photograph of a brick after service is shown in Figure 12. Because of the apparent wear of the brick, it was suspected that corrosion was a cause of failure.



**Figure 12: 90% Al_2O_3 Brick After
Ferrous Foundry Service**

The 90% Al_2O_3 brick was made using fused alumina aggregate bonded in a matrix of mullite and glass. The calcium-iron-alumino-silicate slag dissolved all of the mullite in the immediate hot face of the refractory and showed evidence of solution of the fused alumina aggregate particles (Figure 13). Phases other than corundum (from the fused alumina – labeled “A”) were hercynite (labeled “H”), calcium hexaluminate, and glass. The fused alumina aggregate appears to dissolve in the slag and form hercynite (iron aluminate spinel) at its periphery.

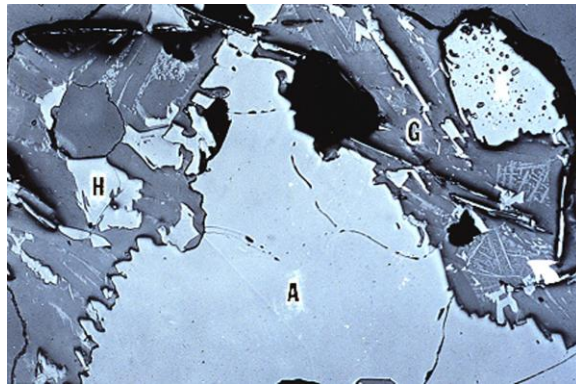


Figure 13: Immediate Slag/Brick Interface Of The Used 90% Alumina Brick (130X)

The slag liquid penetrated the refractory to a depth of 10-20 mm behind the hot face. At a depth of about 8-10 mm behind the hot face, mullite appeared in the microstructure indicating that the CaO content of the penetrating slag dropped below about 8% (Figure 14). In the upper field of this photomicrograph, glass or slag (labeled “G”) penetrated between fused alumina aggregate particles (labeled “A”). Needle-like crystals of calcium hexaluminate are dispersed in the glass phase. In the lower field, mullite (labeled “M”) appears as clusters of individual crystals dispersed in a glass phase somewhat altered in chemistry by the slag penetration.

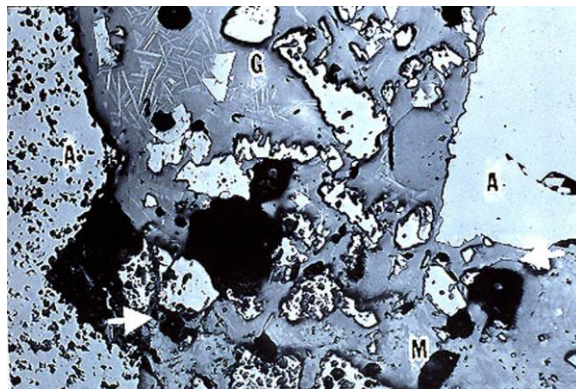


Figure 14: Area Where Mullite Reappears Behind the Hot Face

In this case, it was determined that the corrosion reactions were those normally expected in a ferrous foundry, i.e. chemical solution of the bond phase

of the brick with penetration behind the hot face. Large “veins” of solidified metal were found within the used brick indicating mechanical failure in service followed by metal penetration.

Basic Brick in Steel Making Applications

Introduction

A 90% MgO class fired, pitch impregnated brick was examined after a short campaign in a basic oxygen furnace producing carbon steel. The slag composition can be viewed as a high CaO/SiO₂ ratio liquid containing a substantial amount of iron oxide. Because the major component of the brick was MgO, the ternary system CaO-MgO-SiO₂ can be used to view the corrosion processes as a first approximation (Figure 15).

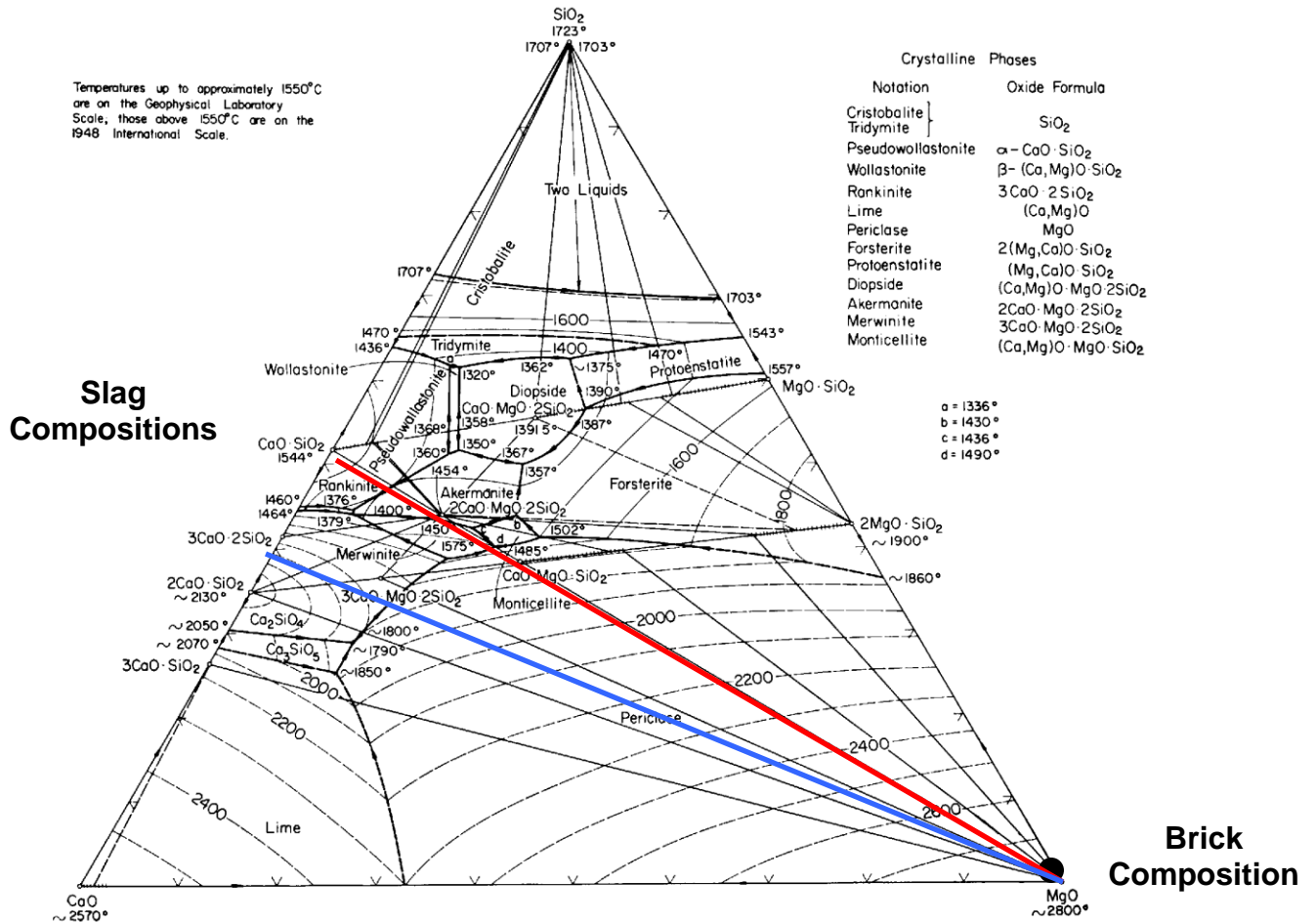


Figure 15: CaO-MgO-SiO₂ Phase Diagram With Illustrations of “Joins” Between Brick (MgO) and Slag (On the CaO-SiO₂ Join)

In the case of the 90% MgO class refractory, the brick contained 95.5% MgO, 2.7% CaO, and 1.4% SiO₂. This implies that the “native” silicate in the brick is dicalcium silicate (2CaO·SiO₂) - a very refractory second phase providing for a

part of the bonding in a product where direct sintered bonds between adjacent MgO aggregate particles predominate. In service, a transient period exists in the steel refining cycle when silicon is being oxidized in the metal bath providing for temporary exposure of the refractory hot face to less basic silicates. This is also a period of enhanced iron oxide contact with the refractory.

Since the refractory composition can be represented by the “MgO” apex on the phase diagram (Figure 15), joins can be drawn to different CaO/SiO₂ ratios illustrating the corrosion process:

- For a CaO/SiO₂ ratio of 1.0, the refractory will react with the slag forming monticellite, CaO·MgO·SiO₂, which melts at 1485°C. An iron-containing analog of monticellite called “iron monticellite” (FeO·MgO·SiO₂) has a melting point of 1230°C. Therefore, corrosion starts above about 1230°C when liquid phases are formed. Slag penetration can result in the disruption of bond phases that are native to the brick lowering the effectiveness of the “bonding silicate phase” in the immediate hot face area.
- For a CaO/SiO₂ ratio of 1.5, merwinite or 3CaO·MgO·2SiO₂ is the reaction product formed in the hot face. Merwinite melts “incongruently” at 1575°C in a process given as:



It is interesting that as the slag basicity increases (i.e. as the CaO/SiO₂ increases), corrosion reactions begin at higher temperature. This is one reason that steel makers wish to have solution of limestone slag additions as early as possible in a refining cycle to retard slag corrosion.

- For a CaO/SiO₂ ratio ≥ 2.0, the lowest eutectic temperature is at ~1790°C. Without considering the iron oxide and other components of the slag, this implies that the reaction product between the slag and the brick is above most steel making temperatures. However, the iron oxide plays an important role significantly reducing the temperature of the reaction products.

The Role of Iron Oxide in Corrosion

The role of iron oxide in corrosion in steel making slag and corrosion is to significantly reduce the melting temperatures predicted by only considering the CaO-MgO-SiO₂ phase diagram. Some of the reaction products commonly found between basic refractories and steel making slag are given in Table 3.

It is immediately obvious that most of the iron containing compounds melt in the area of 1200-1350°C while most of the calcium silicate phases melt

above 1485°C. It is also true that melting can typically begin below these indicated temperatures by as much as 50°C due to the effect of other impurities and due to the presence of multi-component eutectics not seen on three component diagrams.

System CaO-MgO-Al ₂ O ₃ -SiO ₂		System FeO-MgO-Al ₂ O ₃ -SiO ₂	
Mineral	Melting Temperature, °C	Mineral	Melting Temperature, °C
2MgO·SiO ₂ (Forsterite)	1900	FeO·SiO ₂ (Fayalite)	1205
CaO·MgO·SiO ₂ (Monticellite)	1485	FeO·MgO·SiO ₂ (Iron monticellite)	1230
3CaO·MgO·2SiO ₂ (Merwinite)	1575	2CaO·(Fe ₂ O ₃ , Al ₂ O ₃)·SiO ₂ (Iron gehlenite)	1285
2CaO·SiO ₂ (Dicalcium silicate)	2130	FeO·Al ₂ O ₃ ·5SiO ₂ (Iron cordierite)	1210
3CaO·SiO ₂ (Tricalcium silicate)	2070	2CaO·Fe ₂ O ₃ (Dicalcium ferrite)	1489
CaO·Al ₂ O ₃ ·2SiO ₂ (Anorthite)	1553	4CaO·Al ₂ O ₃ ·Fe ₂ O ₃ (Brownmillerite)	1395
2CaO·Al ₂ O ₃ ·SiO ₂ (Gehlenite)	1593	6CaO·2Al ₂ O ₃ ·Fe ₂ O ₃	1365
CaO·Al ₂ O ₃ ·2SiO ₂ and 2CaO·Al ₂ O ₃ ·SiO ₂ (Melilite)	1380		

Table 3: Reaction Products Between Steel Making Slag And Basic Refractories with Melting Points for Full Melting or Partial Melting (Peritectic Reactions)

The corrosion process between calcium-iron-silicate slag and magnesia containing refractories can depend on the mobility and concentration of reactants. A photomicrograph of the immediate slag/brick interface region in a brick from a steel making furnace location *above the metal line* is shown in Figure 16. Here the reaction products are “mixed” iron spinel or (MgO, FeO)·(Al₂O₃, Fe₂O₃), dicalcium silicate (2CaO·SiO₂), and dicalcium ferrite (2CaO·Fe₂O₃). Because of the high concentration of iron oxide dust in the furnace atmosphere and the lack of persistent slag attack (or flow), the spinel phase formed a sort of “barrier coating” over the face of the brick.

By contrast, a brick from a slag line application exhibited a very different corrosion process (Figure 17). Here the products of corrosion appear to be dicalcium ferrite (2CaO·Fe₂O₃) penetrating around individual magnesium oxide crystals (rounded gray crystals) with isolated pockets of black appearing dicalcium silicate (2CaO·SiO₂) present in the slag layer. Magnesium oxide

crystals appear to be eroded from the refractory surface in response to the extremely high temperatures and the intensity of the slag contact.

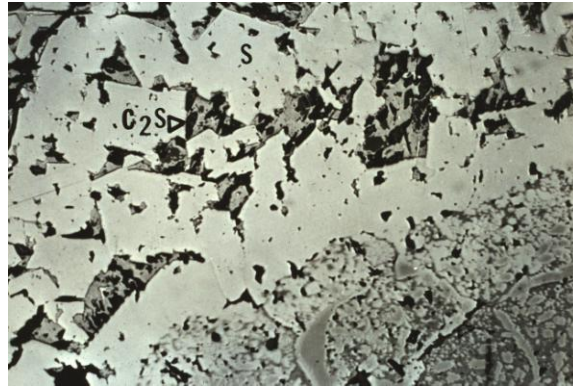


Figure 16: Corrosion Interface in an MgO Brick From an Upper Sidewall Location

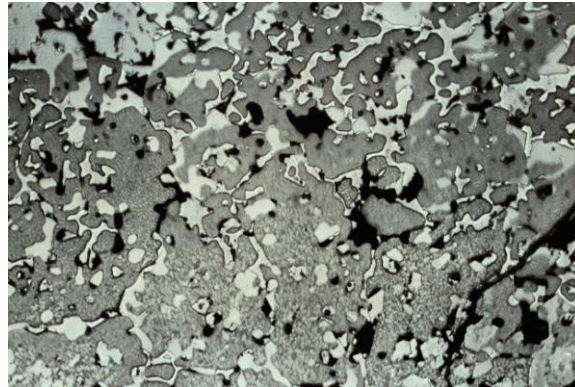
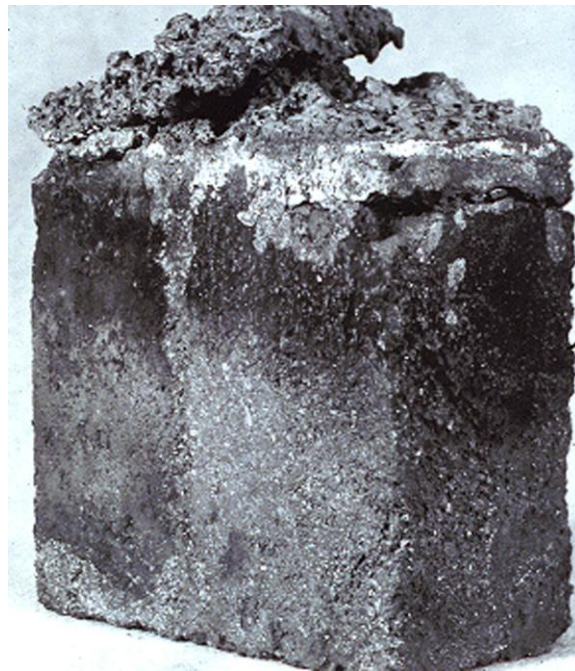


Figure 17: Corrosion Interface in an MgO Brick From a Slag line Location

In these cases, the microstructures at the reaction interface are extremely different despite the fact that the brick were in the same furnace. In the upper sidewall, reaction with iron oxide and lime containing dust contributed to the corrosion process. By contrast, in the slag line, persistent contact with flowing slag caused corrosion and erosion processes to take place.

**Case Study: 90% MgO Burned-Impregnated Brick
After Service in the Basic Oxygen Steel making Furnace**

A typical used brick from a “bottom tuyere pedestal” (also called a “bottom plug”) is shown in Figure 18. The bottom plug contains tuyeres where oxygen is injected into the molten metal bath to facilitate the refining process. The brick are exposed to the localized high temperatures from the exothermic reaction between the oxygen and the metal. It is notable that this brick exhibits a layer apparently in the process of spalling away from the brick hot face.



**Figure 18: 90% MgO Burned Impregnated Brick
After Service in a BOF Bottom Plug**

The hot face region of the brick is shown in Figure 19 at low magnification. The immediate slag/brick interface is in the upper field of the photomicrograph. The slag phase penetrating among individual MgO crystals is dicalcium ferrite forming a thin “dense layer” in the outer zone of the brick. Behind the dense layer, a zone of porosity is noted as ‘black areas’ – areas where the impregnated carbon phase in the brick was removed by oxidization.

Further behind the hot face in Figure 19, a large void is seen in the lower left of the photomicrograph. As will be seen in the following, this void resulted from a defect in the formulation of the brick. With prolonged exposure to heat, the defect in a precursor to the “peeling” away of the surface by spalling as seen in Figure 18.

The corrosion process is seen in a field near the immediate hot face (Figure 20). Here dicalcium ferrite (bright phase) and dicalcium silicate penetrate around individual MgO crystals from aggregate particles. Several smaller rounded MgO crystals are in the final phase of dissolution. Even though dicalcium silicate is a “compatible” phase with MgO, it will still dissolve MgO – as is evident from the photomicrograph. Thus, the corrosion process can, in part, be represented as solution of MgO in $2\text{CaO}\cdot\text{SiO}_2$.

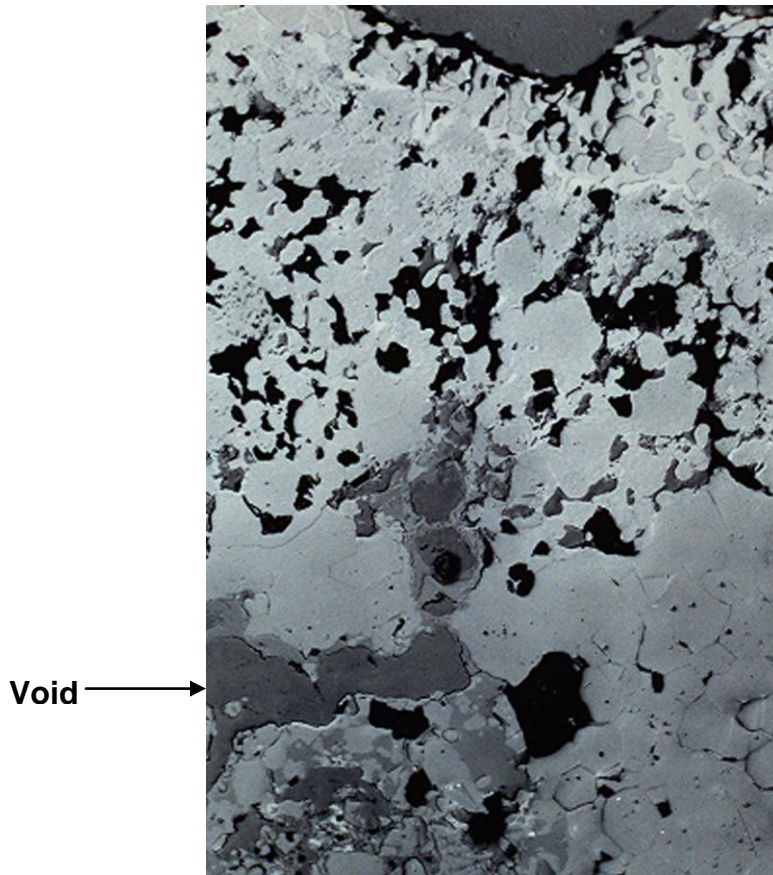


Figure 19: Hot Face Region of The MgO Brick (50X)

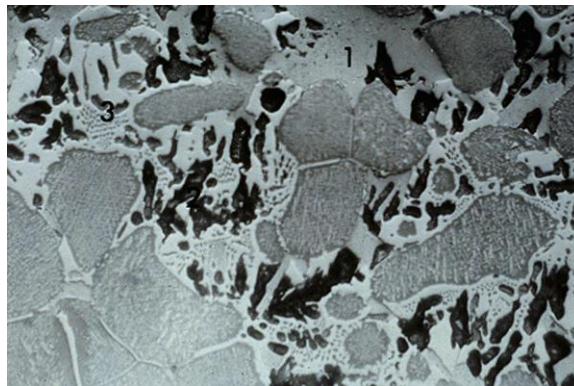


Figure 20: Field in the Hot Face Zone (130X)

Further behind the hot face, a zone was discovered where the “matrix” of fines (and carbon) shrunk away from the aggregate particles (Figure 21). This created voids at the periphery of the coarse aggregate particles in the brick, and these voids eventually consolidated leading to the larger void of Figure 19. These voids lead to the peeling away of layers during service (spalling of thin layers)

causing excessive wear. When confronted with the evidence, the developers of the brick were *amazed* that this separation took place because they had not seen it in laboratory “coking box” experiments. Eventually, the idea was advanced that the coking box temperature of about 1000°C was quite a bit different than the service temperature of the brick ($\geq 1600^\circ\text{C}$).

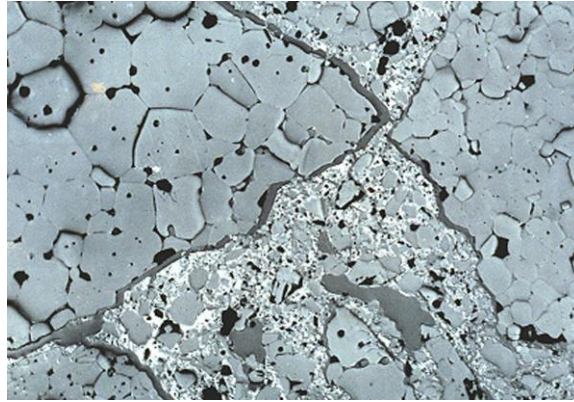


Figure 21:

Magnesia-Chrome Brick in AOD Service

In other case studies, magnesia-chrome and dolomite refractories were examined after service in an argon-oxygen-decarburization (AOD) reactor producing stainless steel. In this instance, slag specimens were collected during typical refining cycles, and bricks were examined after the end of the service campaign.

The AOD refining cycle of slightly over one hour includes an initial period (decarburization cycle) where silicon is oxidized in the metal producing a very viscous or “chunky” slag. A photomicrograph of this early slag shows clusters of spinel phases or $(\text{MgO}, \text{FeO}) \cdot (\text{Cr}_2\text{O}_3 \cdot \text{Al}_2\text{O}_3 \cdot \text{Fe}_2\text{O}_3)$ and bright metal droplets interdispersed in a calcium silicate glass (Figure 22).

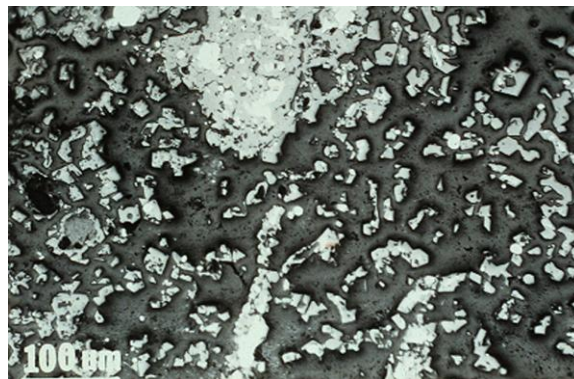


Figure 22: Early AOD Slag (50X)

The angular spinel crystals and metal droplets are shown at higher magnification in Figure 23. The “chunky” nature of the slag is due to the viscosity of the slag created by the high concentration of spinel crystals.

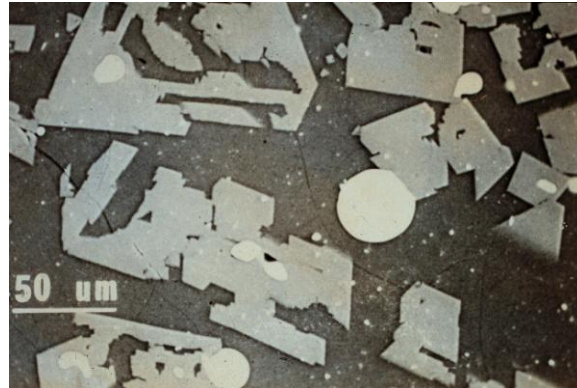


Figure 23: Detail of Early AOD Slag

The early AOD slag also contained eroded masses of MgO crystals. One such fragment can be seen in the lower left field of Figure 22 and in a photomicrograph taken using a scanning electron microscope (Figure 24). In this latter picture, spinel crystals in a continuum of calcium silicate glass surround a dark gray mass of MgO in the center of the photomicrograph.

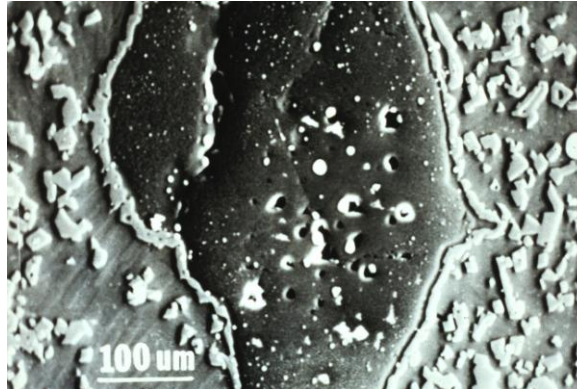


Figure 24: Eroded MgO Mass in Early AOD Slag

The AOD refining cycle also includes a short “reduction period” where argon is injected into the metal to recover chromium from the slag. In effect, the spinel phases are substantially reduced. This cycle also employs an increased slag CaO/SiO₂ ratio to facilitate chromium recovery.

A photomicrograph of a reduction slag is shown in Figure 25. Only a few spinel crystals protrude from the glass indicating high efficiency of reduction. The slag shows sign of water etching during polishing consistent with the solubility of merwinite and/or gehlinite (See Table 3).



Figure 25: AOD reduction Slag (130X)

Fired magnesia-chrome brick were used in early AOD linings. Despite a more recent trend to use magnesia-carbon products in these furnaces, the examination of magnesia-chrome brick illustrates several principles of corrosion processes. One brick from a mid-barrel location in a 50-ton AOD reactor is shown in Figure 26. The continuous glassy slag coating on the hot face is typical for AOD service.

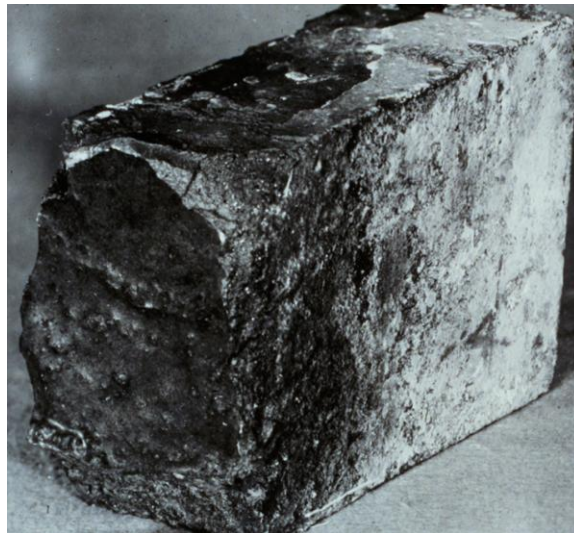


**Figure 26: Used Magnesia Chrome Brick
After AOD Service**

The immediate hot face area of the magnesia-chrome brick is shown in Figure 27. A chromite grain (labeled “Cr”) is in the center of the photomicrographs with a coarse magnesia aggregate particle to the left of the field. The slag layer is at the top of the photomicrograph. It is apparent from the “jagged” nature of the brick surface that the corrosion process has preferentially removed the matrix of the refractory leaving coarse grains to protrude into the slag layer. What appears to be “corrosion” of the periphery of the chromite grains can also be seen at this low magnification.

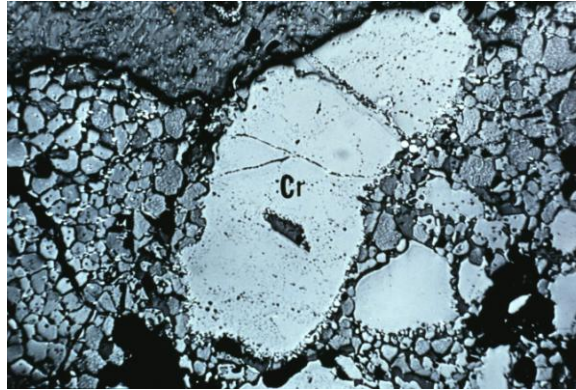


Figure 27: Slag/Brick Interface (50X)

A detailed view of the hot face region is shown in Figure 28 (slag layer toward the top of the field). Here, merwinite or $3\text{CaO}\cdot\text{MgO}\cdot 2\text{SiO}_2$ can be seen toward the top of the field (labeled “m”). The other slag silicate is monticellite or $\text{CaO}\cdot\text{MgO}\cdot\text{SiO}_2$. Both of these are expected as compatible phases for slag in the CaO/SiO_2 range of 1.0-1.5 in contact with MgO containing refractories (See Figure 15).

The corroded appearing edges of the chromite grains are “secondary” spinels that did not exist at the service temperature of the brick in the hot face region. The process was dissolution of the constituents of the chrome ore (Al_2O_3 , Cr_2O_3 , and Fe_2O_3) in the penetrating slag followed by preferential precipitation around the chromite grains on cooling of the lining for the last time. These spinels did not form on the “top” of the chromite grains in the immediate slag/brick interface because of the rapid quenching after the last heat of steel was made. Metal droplets are also seen in Figure 28. These may have formed, in part, due to reduction of oxides in the chromite to the metallic state.

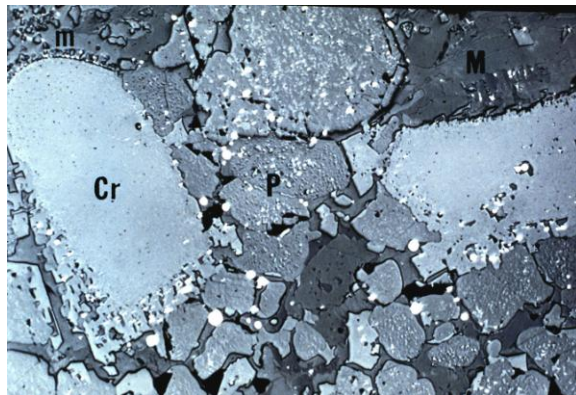


Figure 28: Detail of the Hot Face Region (130X)

The corrosion process can be summarized as follows:

- Solution of MgO in the slag phases, penetration of slag into the brick, and disruption of the direct bonding behind the hot face.
- Solution of chromite in the slag phases and partial chemical reduction of oxides to the metallic state.

In magnesia-chrome brick and other bonded refractories, slag penetration can occur to a depth of 75 mm or more behind the hot face. While significant chemical corrosion is usually limited to a depth of less than about 25 mm behind the hot face, the presence of the slag changes the physical properties of the brick due to shrinkage of the refractory and other processes. If the thermal expansion coefficient in the penetrated zone becomes different than that in the cold face region, spalling can occur near the interface between the penetrated and “un-penetrated” or cold face zones. Used brick can exhibit cracks in this zone and even larger voids where cracks have apparently joined. This phenomenon is called “densification spalling”, and it can result in spalling loss of sections of about 75 mm in thickness.

Dolomite Brick in AOD Service

Dolomite refractories were used in AOD service in the early stages of development of the AOD process. Dolomite brick contain “islands” of MgO crystals in a continuum of CaO. The hot face region of a used dolomite brick after AOD service is shown in Figure 29. In this photomicrograph, the immediate hot face is to the right of the photomicrograph. The central area of the photomicrograph is the affected zone where corrosion has resulted in reaction of slag with the CaO continuum in the brick forming dicalcium silicate and tricalcium silicate (the black phase etched with water in polishing). Metal droplets are apparent in this region. Aside from chemical corrosion, spalling is also known to occur in AOD service.

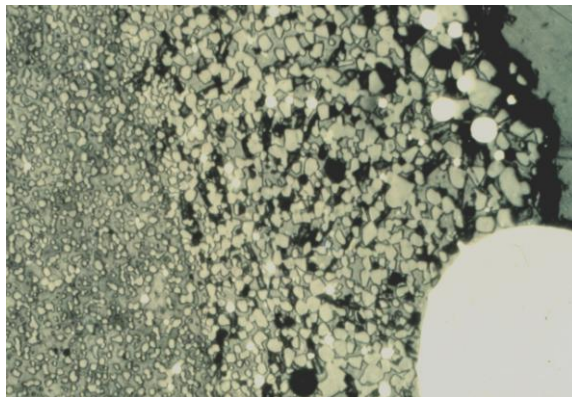


Figure 29: Dolomite Brick After AOD Service (130X)

Gas Phase Reactions

The gas phase in a furnace may be the partial or even sole contributor to corrosion reactions or other deterioration in refractories. Some of the processes that have been recognized include:

1. Alkali transport to refractory surfaces resulting in surface reaction and penetration.
2. Reduction of the refractory and gas phase corrosion.
3. Alternating oxidation and reduction causing sequential dimensional changes in refractories that may enhance spalling.

The potential for alkali to cause “glazing” on the surface has been previously discussed (See Figure 5). It is less well recognized that alkali compounds can volatilize in furnace atmospheres resulting to transport of the volatile species to the surface of the refractory where vapor phase penetration may also occur.

The melting points of sodium and potassium reaction products with alumino-silicate refractories are given in Table 4. The melting points of the phases themselves are not indicative of the very low eutectic temperatures found in the system. For example, the lowest eutectic in the system $\text{Na}_2\text{O}\text{-Al}_2\text{O}_3\text{-SiO}_2$ (Figure 5) is 732°C .

Phase	Melting Point, °C
$\text{Na}_2\text{O}\cdot\text{Al}_2\text{O}_3\cdot 6\text{SiO}_2$ (albite)	1100
$\text{Na}_2\text{O}\cdot\text{Al}_2\text{O}_3\cdot 2\text{SiO}_2$ (carnegite)	1526
$\text{K}_2\text{O}\cdot\text{Al}_2\text{O}_3\cdot 6\text{SiO}_2$ (carnegite)	1220
$\text{K}_2\text{O}\cdot\text{Al}_2\text{O}_3\cdot 4\text{SiO}_2$ (leucite)	1686
$\text{K}_2\text{O}\cdot\text{Al}_2\text{O}_3\cdot 2\text{SiO}_2$ (kaliophilite)	>1700

Table 4: Alkali Phases Found in Used Refractories

The sidewall of a sawdust fired tunnel kiln producing facing brick is shown in Figure 30. In the central section of the picture, the effect of the plume of combustion from the top burner position nearest the wall is seen (kiln draft from left to right). A black slag is seen coating the fireclay brick with white salt deposits visible in this picture taken after seven years of service. There was only surface glazing of the brick in the sidewall of the kiln. Glazing is also shown on the insulating firebrick surface in the crown of the kiln (Figure 31).



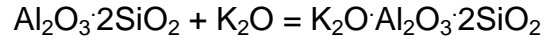
Figure 30: Sidewall of Sawdust Fired Tunnel Kiln After Seven Years of Service



Figure 31: Crown of Sawdust Fired Tunnel Kiln After Seven Years Showing Surface Glazing and Sheet Spalling

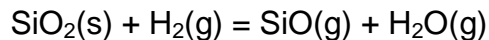
The sidewall brick had expanded due to alkali attack to the point that they were replaced. In addition, the insulating firebrick in the crown exhibited both surface glazing and “sheet” spalling. Sheet spalling is well known, and it usually results from a subsurface expansion reaction caused by penetration of an agent in the gas phase that subsequently reacts with the refractory.

Alkali halides are volatilized in kiln atmospheres. They undergo hydrolysis reactions in a moist high temperature environment forming alkali oxide species. These oxides can cause glazing or expansion. The expansion reaction with potassium is particularly deleterious for refractories with the reaction given as:



where $\text{Al}_2\text{O}_3 \cdot 2\text{SiO}_2$ is metakaolin (a decomposition product of fireclay) and the reaction product is kaliophyllite. The volume expansion due to formation of kaliophyllite is on the order of 15% (linear expansion of ~5%). As potassium is a product of combustion of sawdust, reactions of this type are expected as the cause of the problems in the sidewalls of tunnel kilns fired with sawdust and as the cause of the sheet spalling (Figure 31).

Gas phase corrosion is also known in refractories containing SiO_2 . It has long been recognized that products containing SiO_2 can be “reduced” by hydrogen or by penetration of aluminum metal. The gas phase reduction by hydrogen can be represented as:



where (s) signifies a solid phase and (g) signifies a gaseous phase.

Refractories exposed to hydrogen (or carbon monoxide) can experience gas phase removal of SiO_2 through the process of forming silicon monoxide. For example, at 1000°C a CO/CO_2 ratio of about 10^{-5} will be sufficient to reduce SiO_2 . Mullite reduction and silica loss at temperatures exceeding 1500°C has been seen in petroleum calcining kilns.

Laboratory Slag Tests

Laboratory slag tests have been developed over the years for evaluating corrosion potential. These slag tests range from a “static” cup test to the “dynamic rotary slag test. The terms “static” and “dynamic” refer to whether the slag is stationary or whether it moves over the refractory surface respectively. Some of the test methods are summarized in Table 5. The rotary slag apparatus is shown during a test in Figure 32. The slag is running out of the apparatus into a well while a technician is checking the temperature using an optical pyrometer.

Microscopic studies have shown that the same types of reactions occur in the rotary slag test as in brick examined after service in metallurgical furnaces. The slag/brick interface area in a magnesia-chrome brick from a rotary slag test using a steel making slag is shown in Figure 33.

Test	Type	Reference or Comment
Cup	Static	The test usually consists of a ~50mm diameter hole core drilled or formed into the refractory that is packed with slag and heated to a selected test temperature for a set time. The test only reflects the isothermal reaction and penetration potential between the slag and the refractory.
Drip	Dynamic	Slag drips over a surface with evaluation of the depth of a “notch” cut in the surface by corrosion. The test is described in ASTM C768. The test reflects the isothermal reaction potential between the slag and refractory when there is a constant supply of unreacted or “fresh” slag.
Rotating Spindle	Dynamic	Refractory bars or rods ~25X25X200mm are partially immersed in a crucible containing slag while the specimen is rotating. The test reflects isothermal reaction potential of a flowing slag without a constant supply of “fresh” slag.
Rotary	Dynamic	Beveled refractory shapes (formed by saw cutting) or monolithic materials constitute a lining of a small rotary furnace that is constantly fed with slag. After the test, the specimens are examined for corrosion loss and slag penetration. This test is described in ASTM C768. The test reflects corrosion under a temperature gradient with a constant supply of “fresh” slag.

Table 5: Laboratory Slag Tests



Figure 32: Rotary Slag Test for Refractories

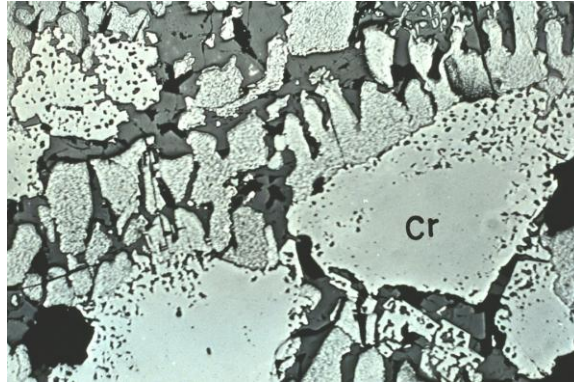


Figure 33: Slag/Brick interface in a Magnesia-Chrome Brick After A Rotary Slag Test

The corrosion process in Figure 33 includes solution of the MgO in the slag consisting primarily of monticellite. The periphery of chromite grains appears to be attacked, but the “porous” spinel phases were formed on recrystallization from the melt when the refractories cooled after the test. The elongated nature of MgO crystals is typical under the influence of the steep temperature gradient in the rotary slag test.

Concluding Comments

Slag corrosion by liquids occurs whenever a threshold temperature is exceeded which is usually when melting occurs between the refractory and the slag. Corrosion results in solution of refractory constituents in the liquid phase resulting in loss of thickness of the refractory lining. The rate of corrosion is dependent on the chemical environment and on the hot face temperature of the refractory.

Models for the corrosion process point to the fact that hot face temperature is the most important variable in controlling refractory life. To reduce corrosion loss, the usual approach is to employ higher purity refractories or lower porosity refractories (such as fusion cast brick) because precise limits on hot face temperature are not practical given process goals. In new furnace designs, consideration should be given to hot face temperature control as a strategy to attain the most economical refractory cost.

Corrosion is primarily a chemical process, and the potential for corrosion can be estimated by reference to phase equilibrium diagrams. These diagrams can allow prediction of the “threshold temperature” for liquid formation. Microscopic techniques allow identification of particular corrosion reactions. Corrosion can also take place through gas phase reactions. The most fundamental way to limit corrosion is to understand the chemical and physical processes involved in corrosion and to formulate strategies to minimize these processes.

Dedication

This chapter is dedicated to the memory of Mr. Walter S. Treffner, the long-time Research Director of the former General Refractories Company (USA). Mr. Treffner was an accomplished microscopist and a dignified researcher in the field of refractories. Mr. Joseph L. Stein, former President of General Refractories (USA), is acknowledged for substantial inspiration on the author's work.

References and Further Reading

C. Burgeron and S. Risbud, Introduction to Phase Equilibria in Ceramics, The American Ceramic Society, Inc., Columbus, OH (1984).

V. G. Konig, Stahl u. Eisen, 91 (2), pp. 63-69 (1971).

R. Herron and C. Beechan, Ceramic Engr. & Sci Proceedings, 2 (11-12), pp. 1126-1140.

K. Endell, R. Fehling, and R. Kley, J. Am. Ceram. Soc., 22, pp. 105-116 (1939).